Anatomic basis of amygdaloid and hippocampal volume measurement by magnetic resonance imaging

C. Watson, F. Andermann, P. Gloor, M. Jones-Gotman, T. Peters, A. Evans, A. Olivier, D. Melanson and G. Leroux

Neurology 1992;42;1743-

Neurorad 1987;8:783-792.
23. Meienberg O, Hoyt WF. Oculomotor control disorder during the neutral phase of periodic alternating nystagmus. J Neurol 1980;223:309-312.
24. Brodal A. Organization of the commissural connections: anatomy. Prog Brain Res 1972;27:167-176.
25. Keane JR. Periodic alternating nystagmus with downward beating nystagmus. Arch Neurol 1974;30:399-402.
26. Towle PA, Romanul F. Periodic alternating nystagmus: first pathologically studied case. Neurology 1970;20:408.
27. Gorman WF, Brock S. Periodic alternating nystagmus in Friedreich's ataxia. Am J Ophthalmol 1950;33:880-864.
28. Leigh RJ, Robinson DA, Zee DS. A hypothetical explanation for periodic alternating nystagmus: instability in the optokinetic-vestibular system. Ann N Y Acad Sci 1981;374:619-635.
29. Furman JMR, Wall C, Pang D. Vestibular function in periodic alternating nystagmus. Brain 1990;113:1425-1439.
30. Waespe W, Cohen B, Raphan T. Dynamic modification of the vestibulo-ocular reflex by the nodulus and uvula. Science 1985; 228:199-202.

Anatomic basis of amygdaloid and hippocampal volume measurement by magnetic resonance imaging

C. Watson, MD, PhD; F. Andermann, MD, FRCP(C); P. Gloor, MD, PhD; M. Jones-Gotman, PhD; T. Peters, PhD; A. Evans, PhD; A. Olivier, MD, PhD, FRCS(C); D. Melanson, MD; and G. Leroux, RT

Article abstract—Both the amygdala and the hippocampus are involved in the pathogenesis of a number of neurologic conditions, including temporal lobe epilepsy, postanoxic amnesia, and Alzheimer's disease. To enhance the investigation and management of patients with these disorders, we developed a protocol to measure the volumes of the amygdala and as much of the hippocampus as possible (approximately 90 to 95%) using high-resolution MRI. We present the anatomic basis of these two protocols and our results in normal control subjects. These volumetric studies of the amygdala may clarify the role of this structure in the pathogenesis of temporal lobe epilepsy.

NEUROLOGY 1992;42:1743-1750

Since the pioneering work of Scoville, Milner, and Penfield,[1-4] many have recognized the critical role of medial temporal lobe structures in declarative or representational memory function. Exactly which structures or combination of structures are crucial for memory continues to be debated. Candidate structures include the hippocampus alone,[5-8] the amygdala alone,[9-11] and both in combination.[12-15] Moreover, in primates, damage to other medial temporal lobe structures such as the entorhinal cortex, perirhinal cortex, and posterior parahippocampal gyrus, either in isolation or in combination with the hippocampus and amygdala, results in memory dysfunction.[15-17] These same medial temporal lobe structures are involved in a number of neurologic conditions, including temporal lobe epilepsy, postanoxic amnesia, and Alzheimer's disease.[6,18-23] As with memory function in the normal state, opinions differ as to the degree, pattern, and necessity of involvement of the various structures, especially the hippocampus and the amygdala.[6,8,11,14,18,19,24-28]

A number of approaches have been utilized to try to clarify these issues, including MRI. Several studies have shown MRI to be superior to CT in the detection of tumors, vascular malformations, and other small lesions causing partial seizures, including those arising from the medial temporal lobe.[29-42] Approximately 60 to 70% of patients with temporal lobe epilepsy, however, have hippocampal sclerosis, which is characterized by neuronal loss and gliosis usually affecting sectors CA1 and CA3 with sparing of CA2, the subiculum, and the dentate gyrus, although occasionally there is more widespread pathology.[18,19,27,28] The success of qualitative MRI in detecting hippocampal sclerosis has varied widely in reported studies,[30,32-35,37,38,40-43] the best results being obtained with a combination of MRI criteria, such as increased signal intensity on T_2-weighted images when that signal is confined to a unilaterally small hippocampus.[44,45]

From the Department of Neurology and Neurosurgery, McGill University, and the Montreal Neurological Institute and Hospital, Montreal, PQ, Canada.

Supported in part by grants MT-10314 awarded to M. Jones-Gotman and R. Zatorre and MA-10160 awarded to A. Evans and T. Peters by the Medical Research Council of Canada. Dr. Watson was supported by a Clinical Fellowship from Sutter Community Hospitals, Sacramento, CA.

Received September 18, 1991. Accepted for publication in final form February 7, 1992.

Address correspondence to Dr. Frederick Andermann, Montreal Neurological Institute, 3801 University Street, Montreal, PQ, Canada H3A 2B4.

There has been recent use of quantitative MRI-based volume measurements of the hippocampus in the study of temporal lobe epilepsy, amnestic patients, Alzheimer's disease, and schizophrenia.[43,46-57] Because each center uses a different method in obtaining results, it is difficult to compare them; indeed certain findings, such as the relative size of the two hippocampi, have varied between groups. Some of these inconsistencies, therefore, may simply represent differences in technique from one center to another.

To obviate many of these discrepancies, we developed a protocol for measuring as much of the hippocampus as feasible. Utilizing the method to be described, we believe that we can reliably measure approximately 90 to 95% of the hippocampus. Because of the importance of distinguishing hippocampal and amygdaloid contributions to the conditions mentioned above, we also developed a protocol to measure the volume of the amygdala in vivo. In this paper we present these two protocols and our initial results in normal control subjects.

Methods. *Subjects.* A total of 21 MRI sequences were obtained from 15 normal control subjects who gave informed consent for the procedure. The subjects were graduate students, residents, fellows, and faculty members at the Montreal Neurological Institute. Medical, neurologic, and IQ examinations were not performed, but none of the subjects gave a history of neurologic or psychiatric symptoms or were taking medications. Six scans were excluded because of poor quality, due primarily to movement artifact. Fifteen scan sequences from 11 subjects were suitable for evaluation. Four subjects were scanned twice, two with different slice thicknesses (one with 2-mm sections, one with 4-mm sections). They afforded an opportunity to test the reliability of the volumetric measurements. The mean age of the 11 subjects was 32.6 years (range, 20 to 59). There were seven men and four women. Ten subjects were right-handed and one left-handed. Handedness was verified using a modification of the Crovitz-Zener handedness questionnaire[58]; probable hemispheric dominance was determined using a dichotic listening test.[59,60]

MR image acquisition. MRI studies were performed on a 1.5-tesla Philips Gyroscan S15-HP unit (Philips International, Eindhoven, Holland). After a scout sequence to insure proper position of the subject's head, a series of sagittal spin-echo images were obtained with 6-mm sections and a 325/20/1 (TR msec/TE msec/number of signal averages) pulse sequence. The plane of the left lateral sulcus was located on the sagittal images, and angled coronal images were obtained perpendicular to this plane. Thirty-two coronal images were obtained using a 3-D gradient-echo fast-field echo (FFE) sequence with 3-mm interleaved (contiguous) sections, a 75/16/2 pulse sequence, a matrix size of 256 × 256, field of vision 250 mm, and 60° flip angle. Additional options were selected as follows: suppression of fold-over artifact in the phase-encoding (superior-inferior) direction and perpendicular regional saturation pulse inferiorly to reduce cervical blood flow artifact. The FFE sequence was chosen in our situation because of improved signal-to-noise and contrast-to-noise ratios per unit time and shortened imaging times compared with conventional spin-echo imaging. A disadvantage of the gradient-echo technique is its vulnerability to image nonuniformity due to static magnetic field inhomogeneity.[61-63]

MR image analysis. The images were transferred to a Sun SPARC 4.1 workstation (Sun Microsystems, Mountain View, CA). Volumetric measurements were performed with an interactive, semiautomated software package developed in the Neuroimaging Laboratory at the Montreal Neurological Institute. The system allows automatic threshold contouring in 2-D and 3-D, manual contouring in 2-D and 3-D, and several other functions, including manual editing of existing regions of interest. In a standard MR image, it is the contrast relationships between pixels, rather than the absolute pixel values themselves, that are meaningful. For this reason, rather than setting the image display level and window at set values across the subject population, the width of the display window was set for each subject to span the range of image values encountered in the temporal lobe area without introducing thresholding effects. In this study, the contours of the hippocampus and amygdala were measured by the same rater (C.W.) to insure consistency, and were performed entirely with the manual contouring function due to the complexity of the structures involved. The mean number of 3-mm slices measured in obtaining the volume of each of the four structures was as follows: (1) right amygdala, 6.27 (range, 6 to 7); (2) left amygdala, 5.55 (range, 5 to 7); (3) right hippocampus, 12.36 (range, 11 to 14); and (4) left hippocampus, 12.18 (range, 11 to 14). Once the outline of the hippocampus or amygdala had been defined, a slice volume was calculated by multiplying the area outlined by slice thickness. The total volume of the structure (amygdala or hippocampus) was then calculated by adding the slice volumes.

Anatomic guidelines. Anatomic guidelines for outlining the amygdala and hippocampus were established using multiple sources, including personal histologic and whole-brain sections prepared by the authors or studied at the Yakovlev Collection (Armed Forces Institute of Pathology, Washington, DC) (C.W. and P.G.), neuroanatomic atlases,[64,65] and frequent correlation with cadaver brain specimens and special dissections by one of us (P.G.). Outlining the boundaries of the amygdala and hippocampus always proceeded from anterior to posterior in a sequential fashion, utilizing the following protocol.

Amygdaloid volume. The amygdala is an ovoid mass of gray matter situated in the superomedial portion of the temporal lobe, partly above the tip of the inferior horn of the lateral ventricle. It occupies the superior part of the anterior segment of the uncus and partially overlies the head of the hippocampus, being separated from that structure by the uncal recess of the inferior horn of the lateral ventricle. On the superomedial surface of the uncus, the amygdala forms a distinct protrusion, the semilunar gyrus, which corresponds to the cortical amygdaloid nucleus. It is separated from the ambient gyrus by the semianular or amygdaloid sulcus, which forms the boundary between the amygdala and the entorhinal cortex. The latter extends into the ambient gyrus and forms most of its surface. The amygdala is separated from the substantia innominata by a deep fold, the endorhinal sulcus, which is lined on the amygdaloid side by the medial nucleus of the amygdala. The superior rim of the ambient gyrus, lying in the fundus of the semianular sulcus, is related to the so-called corticoamygdaloid transition area, which probably represents periamygdaloid cortex. The medial surface of the ambient gyrus often shows a marked indentation, the tentorial indentation (also sometimes called the "uncal notch"[64] or the "intrarhinal sulcus"[66]), produced by the free

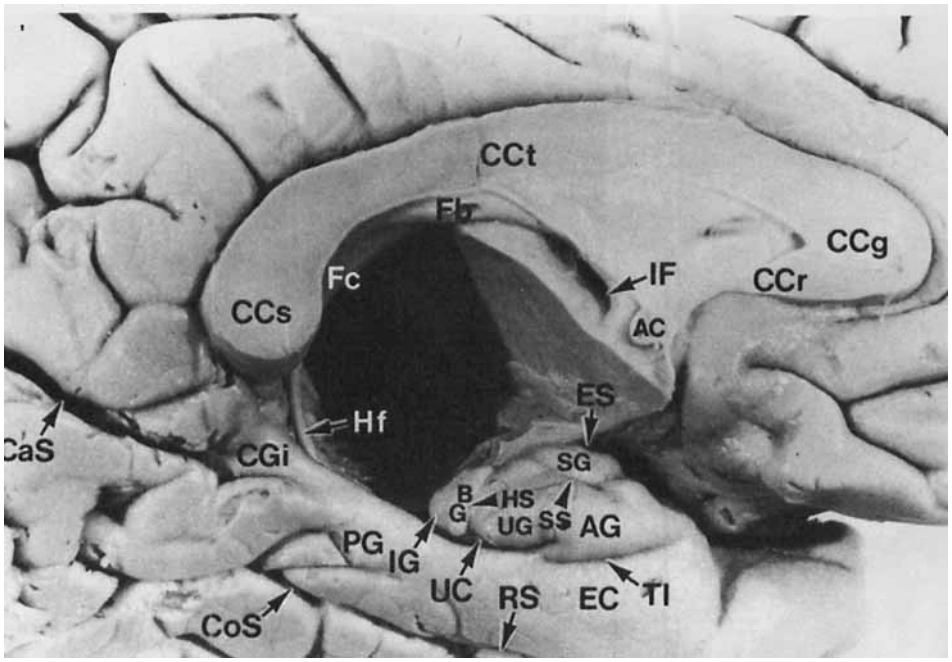

Figure 1. Medial view of the left cerebral hemisphere showing surface anatomy of the medial temporal lobe. A = amygdala; AC = anterior commissure; AG = ambient gyrus; BG = band (limbus) of Giacomini; C = claustrum; CaS = calcarine sulcus; CCg = corpus callosum, genu; CCr = corpus callosum, rostrum; CCs = corpus callosum, splenium; CCt = corpus callosum, trunk; CGi = isthmus of cingulate gyrus; CoS = collateral sulcus; CSi = circular sulcus of insula; EC = entorhinal cortex; ES = endorhinal sulcus; Fb = fornix, body; Fc = fornix, crus; GP = globus pallidus; Hb = hippocampus, body; Hf = fimbria of hippocampus; Hh = hippocampus, head (pes); HS = hippocampal sulcus; Ht = hippocampus, tail; IF = interventricular foramen; IG = intralimbic gyrus; LGB = lateral geniculate body; LVct = lateral ventricle, collateral trigone; LVi = lateral ventricle, inferior horn; OT = optic tract; P = putamen; PG = parahippocampal gyrus; RS = rhinal sulcus; SC = subicular complex; SG = semilunar gyrus; SI = substantia innominata; SS = semianular (amygdaloid) sulcus; TI = tentorial indentation; UC = uncal cleft; UG = uncinate gyrus.

edge of the tentorium cerebelli (figure 1).

The anterior end of the amygdala was arbitrarily and consistently measured on the MRI section at the level of the closure of the lateral sulcus to form the endorhinal sulcus. Although we recognize that this procedure potentially excludes part of the anterior amygdaloid area, we thought that this region was too difficult to visualize reliably on MRI and might well consist of other structures, such as the anterior-inferior extent of the claustrum and the endopyriform nucleus. The medial border of the amygdala is covered by part of the entorhinal cortex, which forms the surface of the ambient gyrus in this region. The entorhinal cortex inferior to the tentorial indentation was excluded from the amygdaloid measurement. If the tentorial indentation was poorly defined or not visible in the anterior amygdaloid region, the line of demarcation between the amygdala and the adjacent entorhinal cortex that occupies the ambient gyrus was defined by a line drawn in direct continuation with the inferior and medial border of the amygdala within the substance of the temporal lobe. By proceeding in this manner, a small amount of the superior extent of the entorhinal cortex will be included in the amygdaloid volume, as is the case when the tentorial indentation is used as the landmark. The inferior and lateral borders of the amygdala were formed by the inferior horn of the lateral ventricle or white matter (figure 2). To define the superior border of the amygdala, we drew a straight line laterally from the endorhinal sulcus to the fundus of the inferior portion of the circular sulcus of the insula. More posteriorly, the optic tract was utilized as a guide to the lateral extension of the crural cistern into the transverse cerebral fissure. This located the medial aspect of the posterior amygdala and was used as the point of departure for defining the medial and superior borders of the structure posteriorly. To define the superior border of the amygdala at this level, a straight line was drawn laterally from the superolateral aspect of the optic tract to the fundus of the inferior portion of the circular sulcus of the insula (figure 3). This method of defining the superior border of the amygdala is arbitrary and undoubtedly excludes small amounts of the medial and central nuclei. However, it should prevent such structures as the substantia innominata, inferior portion of the putamen, and inferior portion of the claustrum from being included in the amygdaloid measurement. At its posterior end, the amygdala occupies the medial half of the roof of the inferior horn of the lateral ventricle, and care must be taken to exclude the tail of the caudate nucleus, the overlying globus pallidus and putamen, and the lateral geniculate body (figure 4). In cases in which the border of the putamen cannot be clearly defined, only the medial half of the structures in the roof should be included in the amygdaloid volume at this level.

Hippocampal volume. The hippocampus is a complex structure consisting of an enlarged anterior part that has been called the "pes," but perhaps is better termed the "head of the hippocampus." This portion of the hippocampus exhibits three or four digitations and turns medially to form the posterior segment of the uncus. As it turns medially, the hippocampus and the dentate gyrus run in the roof of the uncal cleft (also sometimes called the "uncal notch," the "uncal sulcus,"[64] and, erroneously, the "hippocampal sulcus"), the sulcus-like cleft that separates the uncus above from the parahippocampal gyrus below. Once the hippocampus and dentate gyrus reach the medial surface of the uncus, they turn up and form the posterior one-third of the medial and superomedial surface of the uncus. Macroscopically, the dentate gyrus is discernible as a narrow elevation, the band or limbus of Giacomini. This is interposed between the intralimbic gyrus, which forms the posterior pole of the uncus and corresponds to sector CA3 of the hippocampus, and the uncinate gyrus, which extends anterior to the band of Giacomini and corresponds partially to sector CA1 and the subiculum. There is no macroscopically visible border between the uncinate gyrus and the ambient gyrus. The floor of the uncal cleft is formed by the presubiculum (figure 1). The body of the hippocampus curves around the upper midbrain and is concave medially. The anatomy in this region is much less complex. Posteriorly, the hippocampal body tapers into the

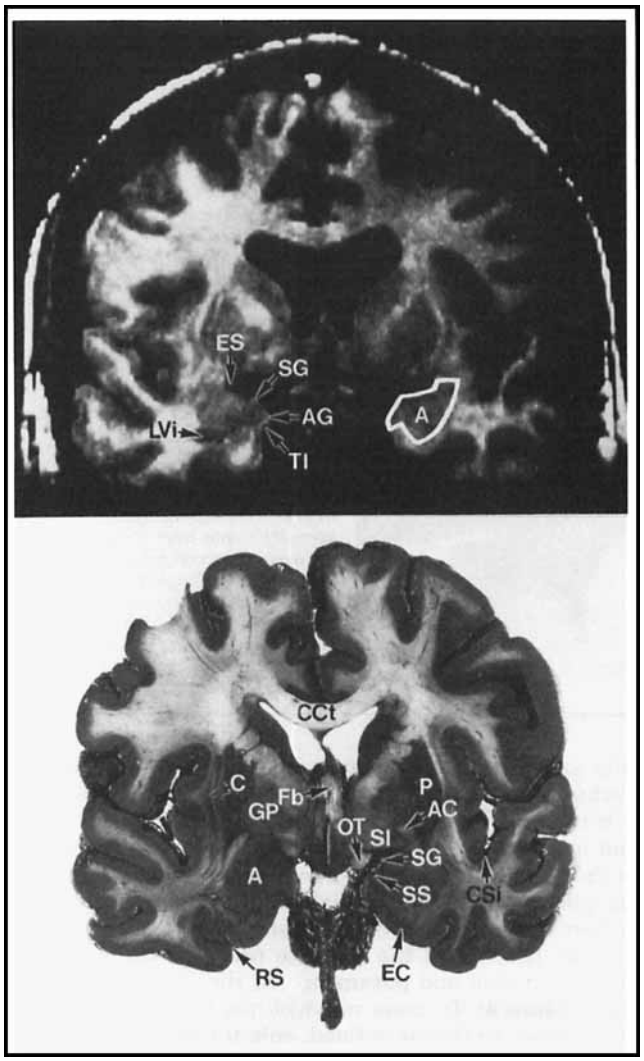

Figure 2. Angled coronal sections of the cerebral hemispheres passing through the anterior segment of the uncus. (Upper plate) MRI with amygdala outlined on the left (see text for MRI sequence variables). (Lower plate) Brain section stained with the LeMasurier modification of the Mulligan stain. For abbreviations, see figure 1 legend.

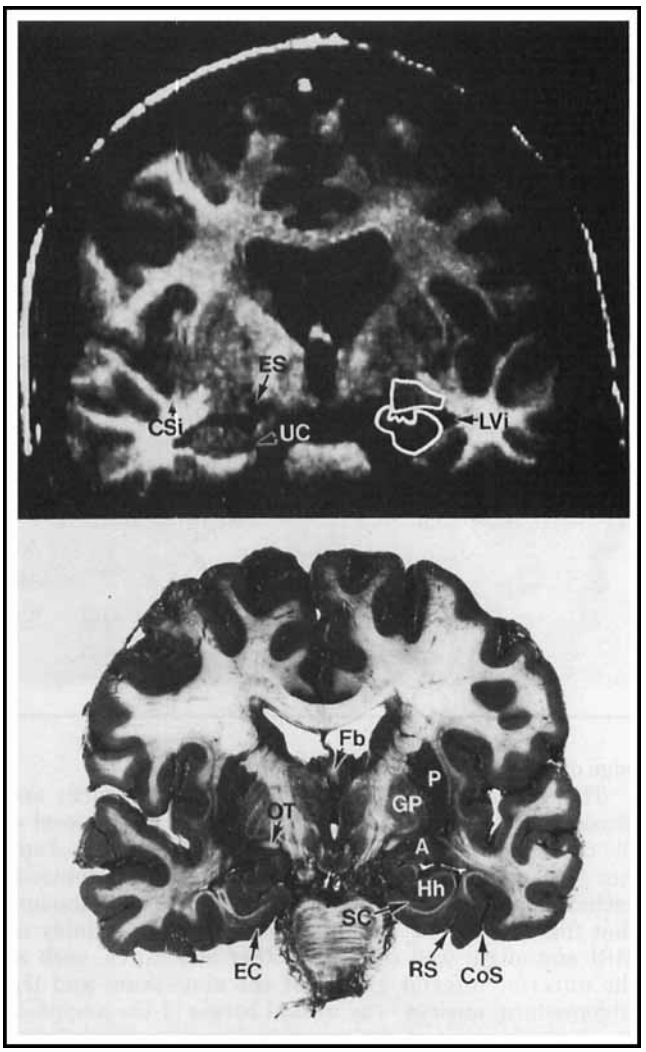

Figure 3. Angled coronal sections of the cerebral hemispheres passing through the posterior segment of the uncus. (Upper plate) MRI with amygdala and hippocampal head outlined on the left. (Lower plate) Brain section. For abbreviations, see figure 1 legend.

tail, which turns medially just anterior to and below the splenium of the corpus callosum. The tail of the hippocampus gives rise to the fasciola cinerea, which ultimately passes around the corpus callosum to continue on its upper surface as the indusium griseum.

It is obviously most difficult to define the boundaries of the hippocampus in its most anterior portion, the hippocampal head. The most reliable structure separating the head of the hippocampus from the amygdala in this region is the inferior horn of the lateral ventricle. This is especially true if the ventricular cavity extends into the deep part of the uncus anterior to the head of the hippocampus, thereby forming the uncal recess of the inferior horn. However, portions of the uncal recess are often obliterated, especially medially, and the hippocampal digitations are fused to the amygdala across the ventricular cavity.[64] When this was the case, three guidelines were used to outline the hippocampal head and separate it from the adjacent amygdala. If an obvious semilunar gyrus was present on the surface of the uncus, a line was drawn connecting the inferior horn of the lateral ventricle to the sulcus at the inferior margin of the semilunar gyrus (ie, the semianular or amygdaloid sulcus). It was also useful to use the alveus covering the ventricular surface of the hippocampal digitations to distinguish the hippocampus from the amygdala. If neither the semianular sulcus nor the alveus was obvious, a straight horizontal line was drawn connecting the plane of the inferior horn of the lateral ventricle with the surface of the uncus. The inferior margin of the hippocampus was outlined to include the subicular complex and the uncal cleft with the border separating the subicular complex from the parahippocampal gyrus being defined as the angle formed by the most medial extent of those two structures. In the normal control population, no attempt was made to outline the gray matter on the superior and inferior banks of the uncal cleft because it was usually quite narrow. The gray matter of the entorhinal cortex or parahippocampal gyrus was excluded from this measurement (figures 3 and 4).

In the hippocampal body, the delineation of the hippocampus included the subicular complex, hippocampus proper, dentate gyrus, alveus, and fimbria. The border between

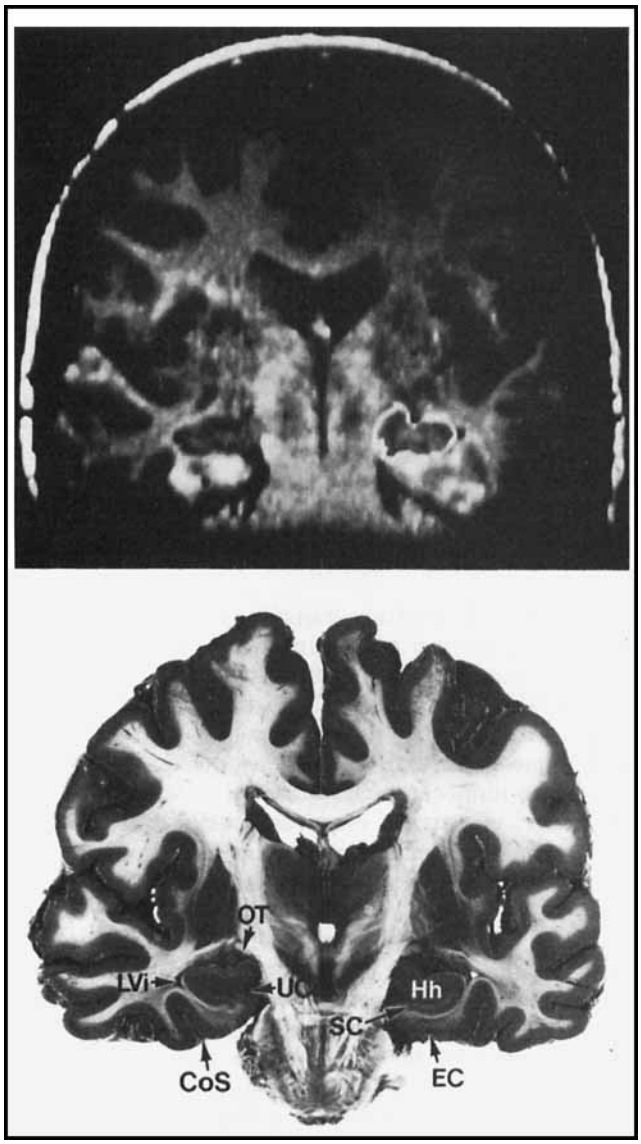

Figure 4. Angled coronal sections of the cerebral hemispheres passing through the posterior segment of the uncus. (Upper plate) MRI with posterior portion of hippocampal head outlined on the left. (Lower plate) Brain section. For abbreviations, see figure 1 legend.

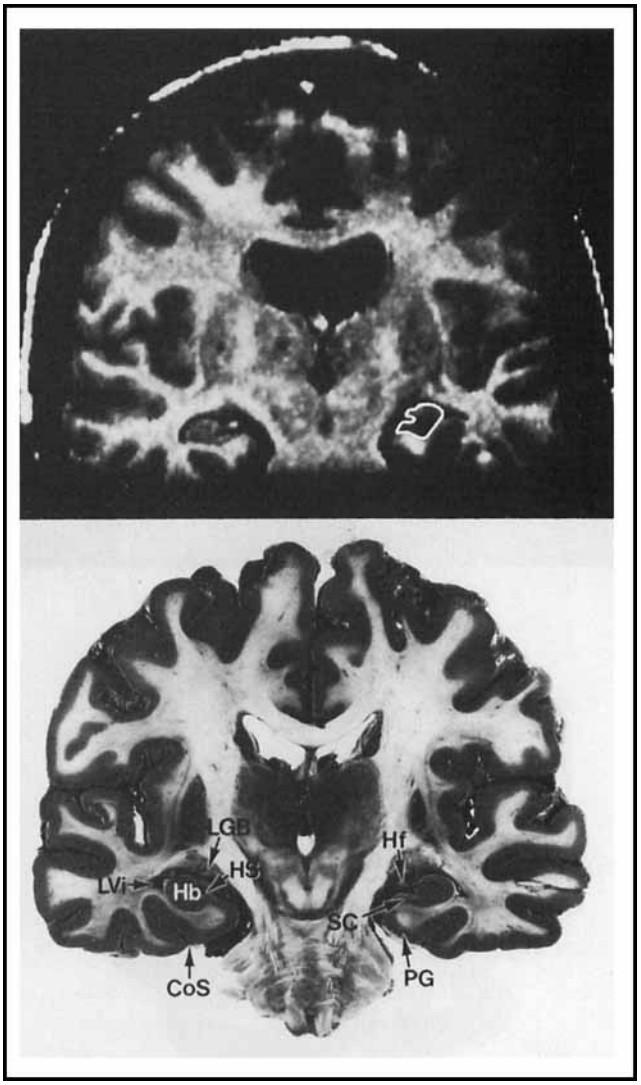

Figure 5. Angled coronal sections of the cerebral hemispheres passing through the lateral geniculate body and the parahippocampal gyrus. (Upper plate) MRI with hippocampal body outlined on the left. (Lower plate) Brain section. For abbreviations, see figure 1 legend.

the subicular complex and the parahippocampal gyrus was defined in the same manner as in the hippocampal head. Therefore, the cortex of the parahippocampal gyrus was once again excluded from the measurement (figure 5).

In the hippocampal tail, measurement again included the subicular complex, hippocampus proper, dentate gyrus, alveus, and fimbria. Excluded at this level were the crus of the fornix, isthmus of the cingulate gyrus (retrosplenial cortex), and parahippocampal gyrus. The most posterior section measured was the section with the crus of the fornix clearly separating from the hippocampus and its fimbria (figure 6). This left a small segment of the tail of the hippocampus outside the measured hippocampal volume.

Since the distance from the anterior end of the hippocampus to the point of separation of the crus of the fornix from the fimbria of the hippocampus was approximately 35 to 38 mm, we estimate that the entire hippocampus except for its most posterior 2 to 4 mm was included in the volume measurement. Therefore, assuming a total anterior-posterior length of the hippocampus of approximately 40 mm,[51,66] these guidelines should result in a volume measurement of 90 to 95% of the total hippocampal formation.

Results. Total volumes of the right and left amygdalae and right and left hippocampal formations as a function of age, gender, and handedness scores are presented in the table. Handedness scores of less than 30 indicate a strong right-handed preference, whereas those greater than 50 are indicative of a left-handed preference. Subject 8 was the only left-handed person in the control group, and therefore his data were not analyzed in the comparison between the right and left amygdaloid and hippocampal volumes. The subject pool was too small to make meaningful comparisons on the basis of age and gender.

Differences between the mean volumes of the right and left amygdalae and the right and left hippocampi for all subjects except no. 8 were com-

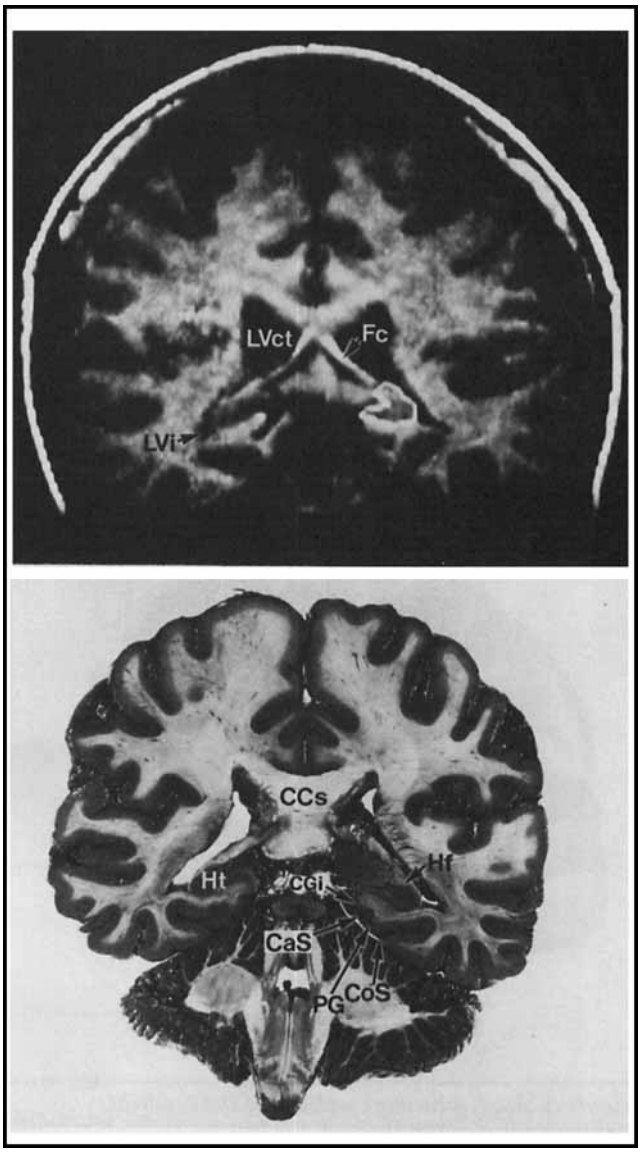

Figure 6. Angled coronal sections of the cerebral hemispheres passing through the splenium of the corpus callosum and isthmus of the cingulate gyrus. (Upper plate) MRI with hippocampal tail outlined on the left. (Lower plate) Brain section showing the transition from fimbria of hippocampus to crus of fornix. (Reproduced with permission from Basic Human Neuroanatomy: An Introductory Atlas, *4th ed, p 167, copyright 1991, Little, Brown and Company.[65]) For abbreviations, see figure 1 legend.*

pared using a paired t test. The right-sided structures consistently were larger than the left, and these differences were statistically significant (t_A = 2.85, p = 0.019; t_H = 4.46, p = 0.0016). In the four subjects who had two MRIs, the differences between the two measurements of amygdaloid volumes were 1 to 5%, and the differences in hippocampal volumes ranged from 1 to 3%. For assessment of test-retest reliability of the volume measurements, the 11 MRIs were remeasured after at least 1 week. Intraclass correlation coefficients for test-retest reliability of left and right amygdaloid and left and right hippocampal volumes ranged from 0.88 to 0.99.

Table. Mean volumes of the amygdalae (A) and hippocampal formations (H) in normal adults

Subject no.	Age/Sex/ Handed score	Right A (mm^3)	Left A (mm^3)	Right H (mm^3)	Left H (mm^3)
1	31/M/24	3,234.33	3,179.88	5,067.48	4,326.96
2	45/M/23	3,470.28	3,303.30	5,238.09	5,143.71
3	28/M/19	3,579.18	3,412.20	6,112.92	5,728.14
4	48/F/25	3,168.99	3,081.87	4,022.04	3,949.44
5	26/F/18	3,165.36	3,121.80	5,027.55	4,239.84
6	28/F/19	3,506.58	3,470.28	5,212.68	4,824.27
7	20/M/21	3,836.91	3,811.50	5,746.29	5,666.43
8	24/M/72	3,277.89	3,256.11	4,541.13	4,501.20
9	25/F/18	3,582.81	3,557.40	5,357.88	4,646.40
10	25/M/24	3,568.29	3,183.51	5,248.98	4,809.75
11	59/M/24	3,488.43	3,459.39	6,327.09	6,098.40
Mean		3,443.55	3,348.84	5,263.83	4,903.14
SD		± 209.47	± 218.61	± 652.33	± 683.64

Discussion. This study indicates that the volume of the amygdala and approximately 90 to 95% of the hippocampus can be measured reliably from high-resolution MRI by utilizing the guidelines mentioned above. Although the differentiation of the amygdala from adjacent structures such as the anterior extension of the hippocampus, putamen, substantia innominata, and claustrum requires special attention, we feel that the criteria employed allow those distinctions to be made in a standardized fashion and with exclusion of a relatively small volume of the structure. The anterior amygdaloid area is especially difficult to measure and is even difficult to define histologically with precision. Therefore, we chose to omit that region in a standardized fashion by beginning our measurement of the amygdala on the most anterior section in which the endorhinal sulcus was present.

The differentiation between the posterior portion of the amygdala and the head of the hippocampus can also be difficult, especially if there is a partial obliteration of the uncal recess of the inferior horn of the lateral ventricle. However, by approaching this region in a standardized fashion, we think that measurement of the two structures is consistent. When measuring the head of the hippocampus, it is important to remember that hippocampal tissue reaches the surface of the brain in the posterior segment of the uncus. Therefore, this area should not be excluded from the measurement of hippocampal volume.

When measuring the most posterior portion of the hippocampus (ie, the hippocampal tail), we chose the intrinsic anatomic relationship of the separation of the crus of the fornix from the hippocampus rather than a fixed anatomic relationship, such as the level of the posterior commissure, for two reasons. First, by choosing a more posterior landmark, we were able to include a larger percentage of the total hippocampal volume. Second, since we intend to utilize this technique to measure post-resection hippocampal volumes in patients undergoing surgery for temporal lobe epilepsy, we were concerned about possible postoperative shifts of the remaining hippocam-

pus and temporal lobe anteriorly that might render assessment inaccurate. The fact that volume measurements in the four subjects who underwent two scanning procedures were almost identical supports the reproducibility of this protocol.

Comparing our results with those from other centers is somewhat difficult, primarily because of different volume measurement protocols.[43,46-57] Our results agree with prior investigations showing the right hippocampus to be larger than the left,[43,50,55] although other studies have not found this asymmetry.[53,54,57] Our results show the right amygdala as well to be somewhat larger than the left, which is in agreement with the findings of Murphy et al[67] made on postmortem material. Our measurement protocol of hippocampal volume most closely approximates that of Jack et al[43,50] in that we attempt to measure the entire hippocampal head as well as the body of the hippocampus. We differ from Jack et al in that we measure the volume of the hippocampal tail as well as the head and body. Other centers restrict their measurements to the region of the hippocampal body, and therefore precise correlation of results may not be possible.[46,51-54,56]

To the best of our knowledge, we are the first to attempt to measure the total amygdaloid volume in a standardized fashion, excluding as little of the structure as possible. A recent investigation[49] measured a partial amygdaloid volume, but because of differences in the extent of measurement our results cannot be compared directly.

The development of high-resolution neuroimaging techniques such as MRI-based volumetric measurement is useful in obtaining in vivo neuroanatomic information in a number of settings, mainly the preoperative evaluation of patients with temporal lobe epilepsy caused by unilateral hippocampal sclerosis. Studies have shown significantly reduced hippocampal volumes, which corroborate neurophysiologic studies and allow lateralization of the epileptogenic region.[43,53-55,57] As experience and information accumulate, we expect that quantitative MRI techniques as well as other neuroimaging studies will reduce the number of patients who require invasive, prolonged, and expensive EEG monitoring, thereby allowing more patients to be treated effectively utilizing noninvasive EEG monitoring coupled with noninvasive imaging techniques and neuropsychological studies.

Quantitative MRI also allows the correlation of preoperative and postoperative amygdaloid and hippocampal volumes with neuropsychological, neuropathologic, and clinical findings.[53-55,68] The addition of amygdaloid volume measurements to those of the hippocampus may allow assessment of the relative contribution of each of these structures to epileptogenesis and memory function. Postoperative quantification of the amount of amygdaloid and hippocampal resection should yield better understanding of which structures need to be removed and in what volume.

Our preliminary data suggest that amygdaloid and hippocampal volume measurements may be helpful in providing supplementary information in patients with bilateral temporal ictal onsets when used in conjunction with EEG, neuropsychological studies, intracarotid amobarbital testing, and PET.[69] The value of quantitative MRI measurements in this group of patients awaits further study and accumulation of a larger normal control group.

References

1. Scoville WB. The limbic lobe in man. J Neurosurg 1954;11:64-66.
2. Milner B, Penfield W. The effect of hippocampal lesions on recent memory. Trans Am Neurol Assoc 1955;80:42-48.
3. Scoville WB, Milner B. Loss of recent memory after bilateral hippocampal lesions. J Neurol Neurosurg Psychiatry 1957;20:11-21.
4. Penfield W, Milner B. Memory deficit produced by bilateral lesions in the hippocampal zone. Arch Neurol Psychiat 1958;79:475-497.
5. Zola-Morgan S, Squire LR. Memory impairment in monkeys following lesions limited to the hippocampus. Behav Neurosci 1986;100:155-160.
6. Zola-Morgan S, Squire LR, Amaral DG. Human amnesia and the medial temporal region: enduring memory impairment following a bilateral lesion limited to field CA1 of the hippocampus. J Neurosci 1986;6:2950-2967.
7. Parkinson JK, Murray EA, Mishkin M. A selective mnemonic role for the hippocampus in monkeys: memory for the location of objects. J Neurosci 1988;8:4159-4167.
8. Sass KJ, Spencer DD, Kim JH, Westerveld M, Novelly RA, Lencz T. Verbal memory impairment correlates with hippocampal pyramidal cell density. Neurology 1990;40:1694-1697.
9. Phillips RR, Malamut BL, Mishkin M. Memory for stimulus-reward associations in the monkey is more severely affected by amygdalectomy than by hippocampectomy [abstract]. Soc Neurosci Abstr 1983;9:638.
10. Murray EA, Mishkin M. Amygdalectomy impairs crossmodal association in monkeys. Science 1985;228:604-606.
11. Tranel D, Hyman BT. Neuropsychological correlates of bilateral amygdala damage. Arch Neurol 1990;47:349-355.
12. Mishkin M. Memory in monkeys severely impaired by combined but not by separate removal of amygdala and hippocampus. Nature 1978;273:297-298.
13. Saunders RC, Murray EA, Mishkin M. Further evidence that amygdala and hippocampus contribute equally to recognition memory. Neuropsychologia 1984;22:785-796.
14. Duyckaerts C, Derouesne C, Signoret JL, Gray F, Escourolle R, Castaigne P. Bilateral and limited amygdalohippocampal lesions causing a pure amnesic syndrome. Ann Neurol 1985;18:314-319.
15. Murray EA, Mishkin M. Visual recognition in monkeys following rhinal cortical ablations combined with either amygdalectomy or hippocampectomy. J Neurosci 1986;6:1991-2003.
16. Zola-Morgan S, Squire LR, Amaral DG. Amnesia following medial temporal lobe damage in monkeys: the importance of the hippocampus and adjacent cortical regions [abstract]. Soc Neurosci Abstr 1988;14:1043.
17. Zola-Morgan S, Squire LR, Amaral DG, Suzuki WA. Lesions of perirhinal and parahippocampal cortex that spare the amygdala and hippocampal formation produce severe memory impairment. J Neurosci 1989;9:4355-4370.
18. Babb TL, Brown WJ. Pathological findings in epilepsy. In: Engel J Jr, ed. Surgical treatment of the epilepsies. New York: Raven Press, 1987:511-540.
19. Bruton CJ. The neuropathology of temporal lobe epilepsy. Oxford, UK: Oxford University Press, 1988.
20. Hirano A, Zimmerman HM. Alzheimer's neurofibrillary changes. Arch Neurol 1962;7:227-242.
21. Hooper MW, Vogel FS. The limbic system in Alzheimer's disease: a neuropathological investigation. Am J Pathol 1976;85:1-20.
22. Herzog AG, Kemper TL. Amygdaloid changes in aging and dementia. Arch Neurol 1980;37:625-629.

23. Hyman BT, Van Hoesen GW, Damasio AR. Memory-related neural systems in Alzheimer's disease: an anatomic study. Neurology 1990;40:1721-1730.
24. Falconer MA, Serafetinides EA, Corsellis JAN. Etiology and pathogenesis of temporal lobe epilepsy. Arch Neurol 1964;10:233-248.
25. Falconer MA. Mesial temporal (Ammon's horn) sclerosis as a common cause of epilepsy: aetiology, treatment and prevention. Lancet 1974;2:767-770.
26. de Lanerolle NC, Kim JH, Robbins RJ, Spencer DD. Hippocampal interneuron loss and plasticity in human temporal lobe epilepsy. Brain Res 1989;495:387-395.
27. Sagar HJ, Oxbury JM. Hippocampal neuron loss in temporal lobe epilepsy: correlation with early childhood convulsions. Ann Neurol 1987;22:334-340.
28. Margerison JH, Corsellis JAN. Epilepsy and the temporal lobes: a clinical, electroencephalographic and neuropathological study of the brain in epilepsy, with particular reference to the temporal lobes. Brain 1966;89:499-530.
29. Aaron J, New PFJ, Strand R, Beaulieu P, Elmden K, Brady TJ. NMR imaging in temporal lobe epilepsy due to gliomas. J Comput Assist Tomogr 1984;8:608-613.
30. McLachlan RS, Nicholson RL, Black S, Carr T, Blume WT. Nuclear magnetic resonance imaging, a new approach to the investigation of refractory temporal lobe epilepsy. Epilepsia 1985;26:555-562.
31. Laster DW, Penry JK, Moody DM, Ball MR, Witcofski RL, Riela AR. Chronic seizure disorders: contribution of MR imaging when CT is normal. AJNR 1985;6:177-180.
32. Sperling MR, Wilson G, Engel J, Babb TL, Phelps M, Bradley W. Magnetic resonance imaging in intractable partial epilepsy: correlative studies. Ann Neurol 1986;20:57-62.
33. Ormson MJ, Kispert DB, Sharbrough FW, et al. Cryptic structural lesions in refractory partial epilepsy: MR imaging and CT studies. Radiology 1986;160:215-219.
34. Lesser RP, Modic MT, Weinstein MA, et al. Magnetic resonance imaging (1.5 tesla) in patients with intractable focal seizures. Arch Neurol 1986;43:367-371.
35. Kuzniecky R, de la Sayette V, Ethier R, et al. Magnetic resonance imaging in temporal lobe epilepsy: pathological correlations. Ann Neurol 1987;22:341-347.
36. Stefan H, Pawlik G, Bocher-Schwarz HG, et al. Functional and morphological abnormalities in temporal lobe epilepsy: a comparison of interictal and ictal EEG, CT, MRI, SPECT and PET. J Neurol 1987;234:377-384.
37. Bergen D, Bleck T, Ramsey R, et al. Magnetic resonance imaging as a sensitive and specific predictor of neoplasms removed for intractable epilepsy. Epilepsia 1989;30:318-321.
38. Heinz ER, Heinz TR, Radtke R, et al. Efficacy of MR vs CT in epilepsy. AJNR 1988;9:1123-1128.
39. Triulzi F, Franceschi M, Fazio F, Del Maschio A. Nonrefractory temporal lobe epilepsy: 1.5-T MR imaging. Radiology 1988;166:181-185.
40. Franceschi M, Triulzi F, Ferini-Strambi L, et al. Focal cerebral lesions found by magnetic resonance imaging in cryptogenic nonrefractory temporal lobe epilepsy patients. Epilepsia 1989;30:540-546.
41. Theodore WH, Katz D, Kufta C, et al. Pathology of temporal lobe foci: correlation with CT, MRI, and PET. Neurology 1990;40:797-803.
42. Brooks BS, King DW, Gammal TE, et al. MR imaging in patients with intractable complex partial epileptic seizures. AJNR 1990;11:93-99.
43. Jack CR, Sharbrough FW, Twomey CK, et al. Temporal lobe seizures: lateralization with MR volume measurements of the hippocampal formation. Radiology 1990;175:423-429.
44. Jackson GD, Berkovic SF, Tress BM, Kalnins RM, Fabinyi GCA, Bladin PF. Hippocampal sclerosis can be reliably detected by magnetic resonance imaging. Neurology 1990;40:1869-1875.
45. Berkovic SF, Andermann F, Olivier A, et al. Hippocampal sclerosis in temporal lobe epilepsy demonstrated by magnetic resonance imaging. Ann Neurol 1991;29:175-182.
46. Seab JP, Jagust WJ, Wong STS, Roos MS, Reed BR, Budinger TF. Quantitative NMR measurements of hippocampal atrophy in Alzheimer's disease. Magn Reson Med 1988;8:200-208.
47. Bogerts B, Ashtari M, Degreef G, Alvir JM, Bilder RM, Lieberman JA. Reduced temporal limbic structure volumes on magnetic resonance images in first episode schizophrenia. Psychiatry Res 1990;35:1-13.
48. Suddath RL, Christison GW, Torrey EF, Casanova MF, Weinberger DR. Anatomical abnormalities in the brains of monozygotic twins discordant for schizophrenia. N Engl J Med 1990;322:789-794.
49. Barta PE, Pearlson GD, Powers RE, Richards SS, Tune LE. Auditory hallucinations and smaller superior temporal gyral volume in schizophrenia. Am J Psychiatry 1990;147:1457-1462.
50. Jack CR, Twomey CK, Zinsmeister AR, Sharbrough FW, Petersen RC, Cascino GD. Anterior temporal lobes and hippocampal formations: normative volumetric measurements from MR images in young adults. Radiology 1989;172:549-554.
51. Press GA, Amaral DG, Squire LR. Hippocampal abnormalities in amnesic patients revealed by high-resolution magnetic resonance imaging. Nature 1989;341:54-57.
52. Squire LR, Amaral DG, Press GA. Magnetic resonance imaging of the hippocampal formation and mammillary nuclei distinguish medial temporal lobe and diencephalic amnesia. J Neurosci 1990;10:3106-3117.
53. Lencz T, McCarthy G, Bronen R, Inserni J, Kim JH, Spencer DD. Hippocampus in temporal lobe epilepsy: correlation of presurgical MRI volumetrics with postsurgical cell counts [abstract]. Epilepsia 1990;31:667-668.
54. Scott T, McCarthy G, Sass K, et al. Hippocampal and temporal lobe MRI volume measurements as an index of memory impairment in patients with temporal lobe epilepsy [abstract]. Epilepsia 1990;31:630.
55. Cascino GD, Jack CR, Parisi JE, et al. Magnetic resonance imaging-based volume studies in temporal lobe epilepsy: pathological correlations. Ann Neurol 1991;30:31-36.
56. Kesslak JP, Nalcioglu O, Cotman CW. Quantification of magnetic resonance scans for hippocampal and parahippocampal atrophy in Alzheimer's disease. Neurology 1991;41:51-54.
57. Ashtari M, Barr WB, Schaul N, Bogerts B. Three-dimensional fast low-angle shot imaging and computerized volume measurement of the hippocampus in patients with chronic epilepsy of the temporal lobe. AJNR 1991;12:941-947.
58. Crovitz HF, Zener K. A group test for assessing hand- and eye-dominance. Am J Psychol 1962;75:271-276.
59. Wexler BE, Halwes T, Heninger GR. Use of a statistical significance criterion in drawing inferences about hemispheric dominance for language function from dichotic listening data. Brain Lang 1981;13:13-18.
60. Zatorre RJ. Perceptual asymmetry on the dichotic fused words test and cerebral speech lateralization determined by the carotid sodium amytal test. Neuropsychologia 1989;27:1207-1219.
61. Frahm J, Haase A, Matthaei D. Rapid three-dimensional MR imaging using the FLASH technique. J Comput Assist Tomogr 1986;10:363-368.
62. Hendrick RE, Kneeland JB, Stark DD. Maximizing signal-to-noise and contrast-to-noise ratios in FLASH imaging. Magn Reson Imaging 1987;5:117-127.
63. Filipek PA, Kennedy DN, Caviness VS, Rossnick SL, Spraggins TA, Starewicz PM. Magnetic resonance imaging-based brain morphometry: development and application to normal subjects. Ann Neurol 1989;25:61-67.
64. Duvernoy HM. The human hippocampus: an atlas of applied anatomy. New York: Springer-Verlag, 1988.
65. Watson C. Basic human neuroanatomy: an introductory atlas. 4th ed. Boston: Little, Brown, 1991.
66. Amaral DG, Insausti R. Hippocampal formation. In: Paxinos G, ed. The human nervous system. New York: Academic Press, 1990:711-755.
67. Murphy GM, Inger P, Mark K, et al. Volumetric asymmetry in the human amygdaloid complex. J Hirnforsch 1987;28:281-289.
68. Hirschorn KA, Jack CR, Marsh WR, et al. Relationship of hippocampal atrophy to postoperative memory performance [abstract]. Epilepsia 1990;31:668-669.
69. Watson C, Andermann F, Gloor P, et al. MRI-based volume measurement of the amygdala and hippocampus: description of method and normal control data [abstract]. Epilepsia 1991;32(suppl 3):76-77.